JOURNAL OF SOLID STATE CHEMISTRY 15, 233–245 (1975)

Vibrational Spectra of Spinels with Cation Ordering on the Octahedral Sites

VASSILIS G. KERAMIDAS,* BERNARDO A. DEANGELIS,† AND WILLIAM B. WHITE‡

Materials Research Laboratory, The Pennsylvania State University, University Park, Pennsylvania 16802

Received October 24, 1974

Infrared and Raman spectra are reported for compounds with 1:1, 1:3, and 1:2 mixed ordering on the octahedral sites of the spinel structure. The spectra of the superstructures are complex with many more bands observed than occur in the parent spinel structure, although less than were predicted by group theoretical analysis. A qualitative interpretation of the spectra can be made through the large Brillouin zone concept.

Introduction

The spinel structure is exceptionally stable and will accept ions with a fairly large range of size and valence states including a broad range of coupled substitutions. Ions from many of the coupled substitutions enter the spinel sites in an ordered way, thus building superstructures on the basic spinel pattern. These include 1:1 ordering on the tetrahedral sites, 1:1, 1:3, and 1:5 ordering on the octahedral sites and a number of mixed ordering schemes. Theoretical aspects of some of these have been considered by Haas (*1*), but the total possibilities are vastly more complex. For example, Billiet et al. (*2*) were able to show by group theoretical and combinational analysis that it is possible to construct 198 superstructures that fit into one of seven space groups based on 1:1 ordering on the octahedral sites alone!

The vibrational spectra of spinels with 1:1 order on the tetrahedral sites were described in an earlier paper (*3*). A different interpretation of the assignments for these spinel types has been published by Tarte and Preudhomme (*4*).

In the present paper, we consider the vibrational spectra of some spinels with several ordering schemes on the octahedral sites. Our approach is first to make a group theoretical analysis of the ordered structures as a means of predicting the number of IR and Raman-active modes. Whether the predicted modes appear in the spectra or not depends on the strength of coupling between the components of the ordered cell and on other dynamic factors. The spectra of some representative ordered structures are then presented and compared with the theoretical predictions.

Theoretical Analysis

The ordering schemes selected for study are listed in Table I. The specific compounds chosen to illustrate these superstructures are listed in Table II with crystallographic data.

The parent spinel structure is cubic and the degrees-of-freedom of the 14 atoms in the primitive unit cell are distributed among the irreducible representations of factor group O_h. Factor group analysis (*10*) predicts that only

* Present address: Bell Laboratories, Murray Hill, N.J. 07974.

† Present address: SNAM PROGETTI SpA, Centro di Richerche di Monterotondo, Rome, Italy.

‡ Also affiliated with the Department of Geosciences.

TABLE I

SPACE GROUPS AND SITE DISTRIBUTIONS FOR OCTAHEDRAL ORDERING SCHEMES

	Spinel	1:1 (α)	1:1 (β)	1:3	1:2 on oct. + 1:2 on tet.
Space group	$Fd3m$ O_h^7	$P4_122$ D_4^3	$Imma$ D_{2h}^{28}	$P4_332$ O^6	$Imma$ D_{2h}^{28}
Example	$[Cr_2]^{VI}[Mg]^{IV}O_4$	$[Li][Nb]^{VI}[Zn]^{IV}O_4$	$[Li][Sb]^{VI}[Zn]^{IV}O_4$	$[Li_{0.5}Al_{1.5}]^{IV}$-$[Al]^{IV}O_4$	$[(TiGa_{0.33})$-$(Li_{0.67})]^{VI}$-$[Ga_{0.67}Li_{0.33}]^{IV}O_4$
Z[a]	8	4	4	8	12

[a] To facilitate comparisons, all formulas are written with respect to four oxygens. The cell contents express the number of these units in the crystallographic cell.

9 of the 17 normal modes will be measurable by vibrational spectroscopy.

$$\text{Raman-active} = A_{1g} + E_g + 3T_{2g}$$
$$\text{IR-active} \quad = 4T_{1u}$$

These predictions are in good agreement with the IR (*11*) and Raman (*12*) spectra of many spinels.

If the octahedral cations order in a 1:1 arrangement, a variety of superstructures are possible (*2*). The ordering called type (α) by Haas (*1*) is tetragonal with twice as many atoms in the primitive unit cell as the parent spinel. The ordered cell parameters are related to those of the spinel by

$$a\,(\text{ordered} \cong a_o/2^{1/2}$$
$$c\,(\text{ordered} \cong a_o$$

TABLE II

CRYSTALLOGRAPHIC DATA FOR ORDERED SPINELS

Compound	a_o (Å)	b_o (Å)	c_o (Å)	References
1:1 order of type (α)				
$LiNbZnO_4$	6.079	—	8.401	This work
$TiZn_2O_4$	6.005	—	8.415	(*5*)
1:1 order of type (β)				
$LiSbCoO_4$	6.054	18.15	8.571	(*6*)
$LiSbZnO_4$	6.026	18.02	8.528	This work
1:3 order				
$LiAl_5O_8$	7.907	—	—	(*7*)
$LiFe_5O_8$	8.33	—	—	(*6*)
$LiGa_5O_8$	8.221	—	—	(*8*)
1:2 mixed order				
$LiGaTiO_4$	5.86	17.59	8.29	(*9*)

The site population in space group $P4_122$ is (*5*):

4 Li^+	on	4(*a*)	C_2
4 Nb^{5+}	on	4(*b*)	C_2
4 Zn^{2+}	on	4(*c*)	C_2
8 O(1)	on	8(*d*)	C_1
8 O(2)	on	8(*d*)	C_1

A factor group analysis presented earlier (*10*) is summarized in Table III. (A discussion and technique for factor group analysis of arbitrarily complex structures has been given by DeAngelis et al. (*13*).) Because of the larger cell and lower symmetry, the number of IR-active modes is 31 and the number of Raman-active modes is 50. All sublattices are represented in all species. Therefore, all unit cell motions are strongly mixed and no attempt has been made to separate quasimolecular vibrations of the BO_4 tetrahedron from the other motions of the unit cell.

TABLE III

ALLOWED MODES AND SELECTION RULES FOR SPINELS WITH TYPE (α) 1:1 ORDERING ON THE OCTAHEDRAL SITES

D_4	Total modes	Acoustic modes	Vibrational modes	Selection rules
A_1	9	0	9	Raman
A_2	12	z	11	IR $E \parallel C$
B_1	10	0	10	Raman
B_2	11	0	11	Raman
E	21	(x, y)	20	IR $E \perp C$ + Raman

TABLE IV

ALLOWED MODES AND SELECTION RULES FOR SPINELS WITH TYPE (β) 1:1 ORDERING ON OCTAHEDRAL SITES

D_{2h}	Total modes	Acoustic modes	Vibrational modes	Selection rules
A_g	5		5	Raman, α_{ii}
B_{1g}	2		2	Raman, α_{xy}
B_{2g}	4		4	Raman, α_{xz}
B_{3g}	4		4	Raman, α_{yz}
A_u	4		4	Inactive
B_{1u}	9	z	8	IR, $E \parallel c$
B_{2u}	7	y	6	IR, $E \parallel b$
B_{3u}	7	x	6	IR, $E \parallel a$

The ordering called type (β) by Haas (*1*) is orthorhombic, space group *Imma*. This is the ordering arrangement in the low temperature form of magnetite where the site population is

4 $Fe^{3+}(IV)$	on 4(*e*)	C_{2v}
4 $Fe^{3+}(VI)$	on (4(*b*)	C_{2h}
4 $Fe^{2+}(VI)$	on 4(*d*)	C_{2h}
8 O(1)	on 8(*h*)	C_s
8 O(2)	on 8(*i*)	C_s

There are four formula units in the body-centered cell and thus the same number of atoms in the primitive cell as in the parent spinel. The factor group analysis is given in Table IV. Because of the lower symmetry which lifts degeneracy and relaxes selection rules, there are 20 IR modes and 15 Raman-active modes.

The 1:3 cation ordering on the octahedral site is exceptionally interesting because the unit cell remains cubic. The octahedral cations

TABLE V

FACTOR GROUP ANALYSIS AND SELECTION RULES FOR SPINELS WITH 1:3 ORDERING ON OCTAHEDRAL SITES

0	Total modes	Acoustic modes	Translatory modes	Rotatory modes	Internal modes of BO_4	Selection rules
A_1	6	—	2	1	3	Raman
A_2	8	—	4	1	3	Inactive
E	14	—	6	2	6	Raman
T_1	22	(x, y, z)	9	3	9	IR
T_2	20	—	8	3	9	Raman

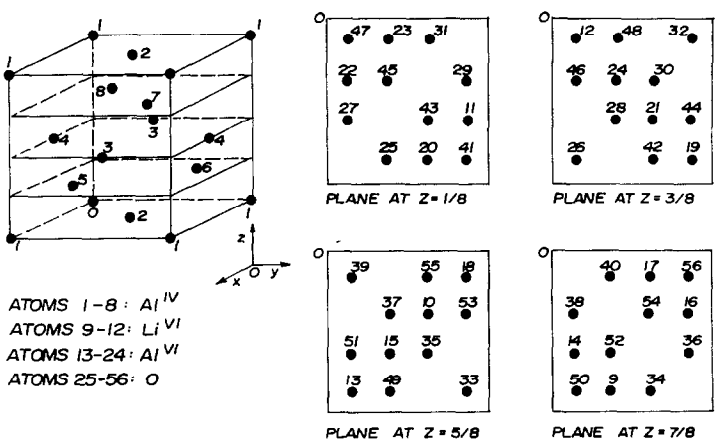

Fig 1. Coordinate system and atom labeling for symmetry coordinates of 1:3 ordered spinels.

in spinel reside on the centers of symmetry and their nonequivalence in the ordered structure removes this symmetry element, lowering the factor group from O_h to O. Ordering also destroys the face-centering operations and the ordered structure has a primitive unit cell the same size as the face-centered cell of the parent structure. The site distribution is

4 Li^+	in 4(*a*)	D_3
12 Al^{3+}(*VI*)	in 12(*d*)	C_2
8 Al^{3+}(*IV*)	in 8(*c*)	C_3
8 O^{-2}	in 8(*c*)	C_3
24 O^{-2}	in 24(*e*)	C_1

Factor group analysis of the ordered structure gives the results shown in Table V. A calculation has been made of the quasimolecular modes of the BO_4 tetrahedron but, as will be seen, these are not particularly useful. The analysis predicts 21 IR-active modes and 40 Raman-active modes with no coincidences. A calculation of the distribution of the degrees of freedom of the individual sublattices shows that the Li^+ atoms (D_3 sites) do not take part in the totally symmetric modes A_1. Otherwise, all sublattices are represented in all species, again suggesting very complex motions.

Although the derivation of the symmetry co-ordinates is cumbersome, due to the large number of atoms in the unit cell, it is interesting to look at those of species A_1. The labeling of the atoms is defined in Fig. 1. The expressions for the six A_1 symmetry coordinates were derived from the symmetry coordinates of the parent spinel structure as given by DeAngelis (*14*) and are listed in Table VI. The A_1 modes, as the A_{1g} modes in spinel, maintain the point symmetry of the unit cell. In the case of the 1:3 ordered structure the point symmetry is D_3, considerably lower than the factor group O, since the space group $O^6(P4_332)$ is nonsymmorphic.

A_1^1 is a motion of the eight tetrahedral Al atoms along one of the bonds. (The tetrahedral bonds are directed along [111].) A_1^6 is a motion of eight oxygen atoms, one for each AlO_4 tetrahedron along [111]. A_1^1 and A_1^6 can be combined to give a stretching mode (one oxygen and the cation move with opposite phase), and a deformation mode (one oxygen and the cation move in phase along [111]).

A_1^3, A_1^4, A_1^5 are motions of the 24 oxygens, three for each AlO_4 tetrahedron, that do not take part in A_1^6; the three modes are partly tetrahedral deformations and partly octahedral stretchings, since the oxygens move along the octahedral bonds.

A_1^2 is a deformation motion of the twelve Al on the octahedral sites along [110], [101] and [011]. From the A_1 symmetry coordinates it can be seen that one tetrahedral bond behaves differently from the other three, thus locally destroying the cubic symmetry. The absence

TABLE VI

SYMMETRY COORDINATES FOR A_1 MODES OF 1:3 ORDERED SPINELS

A_1^{1a}	$\frac{1}{2(6)^{1/2}}$	$[x_1 - x_2 - x_3 + x_4 - x_5 - x_6 + x_7 + x_8 - y_1 - y_2 + y_3 + y_4 + y_5 - y_6 + y_7 - y_8 - z_1 + z_2 - z_3 + z_4 + z_5 - z_6 - z_7 + z_8]$
A_1^2	$\frac{1}{2(6)^{1/2}}$	$[x_{13} + x_{14} + x_{16} + x_{18} - x_{20} - x_{21} - x_{23} - x_{24} + y_{13} + y_{15} - y_{16} - y_{17} + y_{19} + y_{21} - y_{22} - y_{23} + z_{14} + z_{15} - z_{17} - z_{18} - z_{19} - z_{20} + z_{22} + z_{24}]$
A_1^3	$\frac{1}{2(6)^{1/2}}$	$[x_{25} + x_{30} - x_{36} - x_{39} + x_{43} + x_{48} - x_{50} - x_{53} - y_{26} + y_{29} - y_{35} + y_{40} - y_{44} + y_{47} - y_{49} + y_{54} - z_{27} + z_{32} + z_{34} - z_{37} + z_{41} - z_{46} - z_{52} + z_{55}]$
A_1^4	$\frac{1}{2(6)^{1/2}}$	$[x_{26} + x_{29} - x_{35} - x_{40} - x_{41} - x_{46} + x_{52} + x_{55} - y_{27} + y_{32} - y_{34} + y_{37} + y_{43} - y_{48} + y_{50} - y_{53} - z_{25} + z_{30} + z_{36} - z_{39} - z_{44} + z_{47} + z_{49} - z_{54}]$
A_1^5	$\frac{1}{2(6)^{1/2}}$	$[x_{27} + x_{32} - x_{34} - x_{37} - x_{44} - x_{47} + x_{49} + x_{54} - y_{25} + y_{30} - y_{36} + y_{39} + y_{41} - y_{46} + y_{52} - y_{55} - z_{26} + z_{29} + z_{35} - z_{40} - z_{43} + z_{48} + z_{50} - z_{53}]$
A_1^6	$\frac{1}{2(6)^{1/2}}$	$[x_{28} + x_{31} - x_{33} - x_{38} + x_{42} + x_{45} - x_{51} - x_{56} - y_{28} + y_{31} - y_{33} + y_{38} - y_{42} + y_{45} - y_{51} + y_{56} - z_{28} + z_{31} + z_{33} - z_{38} + z_{42} - z_{45} - z_{51} + z_{56}]$

[a] The superscripts merely provide a label for the six independent coordinates. The coordinates x, y, z refer to displacements Δx, Δy, and Δz along the cartesian coordinate axes.

of cubic symmetry in the A_1 modes can be observed over the whole cell and the conservation of the D_3 symmetry is apparent.

The 1:3 ordered structure is still cubic and one would expect that the A_{1g} mode of O_h^7 would be practically unchanged in O^6. In reality the form of the A_{1g} mode is completely absent from the A_1 modes of O^6. Our use of the terms "stretching" and "bending" in the communication on spinels with 1:1 order on the tetrahedral sites (*3*) was heavily criticized by Tarte (*4*) as being totally inadequate to describe highly coupled systems. It should be apparent from the above as well as in the earlier paper that the vibrational motions are described by the symmetry coordinates. Use of such terms as "stretching" and "bending" serves only as a convenient label.

The structure of $LiGaTiO_4$ has one of the most complex ordering schemes that has been described in some detail (*9*). There is 1:2 ordering of a random distribution of ($3Ti^{4+}$ + Ga^{3+}) with $2Li^+$ on the octahedral sites and a 1:2 ordering of $2Ga^{3+}$ with Li^+ on the tetrahedral sites. The resulting structure is orthorhombic with 12 formula units in the body-centered cell. The relation of the cell edges to the parent spinel are

$$a\ (\text{ortho}) \cong a_0/2^{1/2}$$
$$b\ (\text{ortho}) \cong 3a_0/2^{1/2}$$
$$c\ (\text{ortho}) \cong a_0$$

The site distribution in *Imma* (D_{2h}^{28}) is

VI	6 Ti^{4+}+2Ga^{3+}	in	8(*h*)	C_s
	6 Ti^{4+}+2Ga^{3+}	in	8(*g*)	C_2
	4 Li^+(1)	in	4(*b*)	C_{2h}
	4 Li^+(2)	in	4(*d*)	C_{2h}
IV	8 Ga^{3+}	in	8(*h*)	C_s
	4 Li^+(3)	in	4(*e*)	C_{2v}
	16 O^{-2}(1)	in	16(*j*)	C_1
	8 O^{-2}(2)	in	8(*h*)	C_s
	8 O^{-2}(3)	in	8(*h*)	C_s
	8 O^{-2}(4)	in	8(*h*)	C_s
	8 O^{-2}(5)	in	8(*i*)	C_s

TABLE VII

ALLOWED MODES AND SELECTION RULES FOR SPINEL WITH 1:2 ORDERING ON BOTH THE OCTAHEDRAL AND TETRAHEDRAL SITES

D_{2h} species	N_{total}	Acoustic modes	Vibrational modes	Selection rules
A_g	17		17	Raman, α_{ll}
B_{1g}	11		11	Raman, α_{xy}
B_{2g}	12		12	Raman, α_{xz}
B_{3g}	17		17	Raman, α_{yz}
A_u	12		12	Inactive
B_{1u}	22	z	21	IR, $E \parallel c$
B_{2u}	19	y	18	IR, $E \parallel b$
B_{3u}	16	x	15	IR, $E \parallel a$

A factor group analysis of the vibrational motions is given in Table VII. The analysis predicts 54 IR-active modes and 57 Raman-active modes. Because of the centrosymmetric cell there is mutual exclusion between the IR- and Raman-active vibrations.

Experimental Methods

Four spinels with 1:1 ordering on the octahedral sites and one spinel with 1:2 ordering on both octahedral and tetrahedral sites [$LiGaTiO_4$] were prepared by solid state reactions. The corresponding oxides and

TABLE VIII

Composition	Raw materials	Sintering conditions
$LiSbCoO_4$	Li_2CO_3, $CoCO_3$, Sb_2O_3	20 hr at 1000°C in air
$LiSbZnO_4$	Li_2CO_3, ZnO, Sb_2O_3	20 hr at 1000°C in air
$LiNbZnO_4$	Li_2CO_3, ZnO, Nb_2O_5	10 hr at 1000°C in air
$TiZn_2O_4$	TiO_2, ZnO	25 hr at 1000°C in air
$LiGaTiO_4$	Li_2CO_3, Ga_2O_3, TiO_2	2 days at 1000°C in air; ordered form obtained by cooling to 600°C at a rate of 5°C/hr

TABLE IX

Composition	Raw materials	Preparation	Sintering conditions
$LiAl_5O_8$	$LiNO_3$ $Al(NO_3)_3 \cdot 9H_2O$	Mixture of raw materials washed in 1:1 solution of $NH_4OH:H_2O$. Resulting gel was dehydrated at 600°C. Mixture sealed in Pt tube	Ordered form: 10 hr at 1270°C; quenched in H_2O. Disordered form; heated at 1350°C
$LiFe_5O_8$	$LiNO_3$ $Fe(NO_3)_3 \cdot 9H_2O$	Mixture of raw materials washed in 1:1 solution of $NH_4OH:H_2O$. Resulting gel was dehydrated at 600°C	Ordered form: 10 hr at 700°C. Disordered form: sealed in Pt tube heated at 900°C; quenched in H_2O
$LiGa_5O_8$	$LiNO_3$ Ga_2O_3	Powders were ground together in an agate mortar. Heated at 600°C to decompose $LiNO_3$	Ordered form: 10 hr at 1050°C in a sealed Pt tube

carbonates were mixed in the correct stoichiometric ratios, ground in an agate mortar, prefired at 600°C for about 5 hr for the decomposition of the carbonates, and finally sintered at 1000°C in air atmosphere. The details are given in Table VIII.

The X ray diffraction powder patterns of $LiSbCoO_4$ and $LiSbZnO_4$ were generally in agreement with patterns computer-generated from literature unit cell parameters (*6*). However, a number of weak reflections could be better indexed on an orthorhombic cell with the parameters listed in Table II. These patterns are consistent with space group *Imma*.

The results for $TiZn_2O_4$ and $LiGaTiO_4$ are in agreement with those reported in the

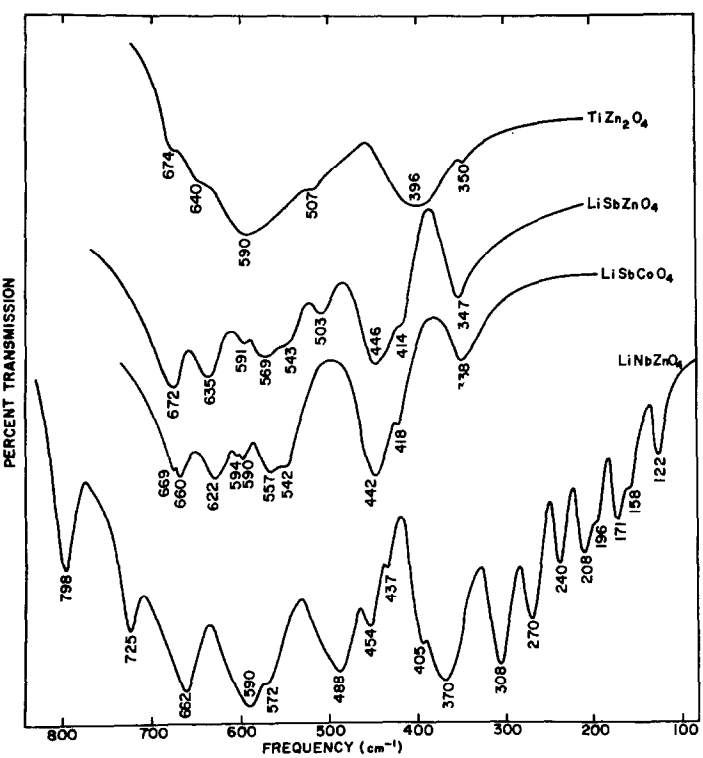

Fig. 2. IR spectra for Spinels with 1:1 order on the octahedral sites.

literature (*9*, *15*). Regarding $LiNbZnO_4$, there seems to be some disagreement about the lattice parameters. There are two sets of values reported: $a_o = 6.08$, $c_o = 8.40$ (*6*) and $a_o = 6.098$, $c_o = 8.427$ (*15*). Using the computer program, d values were calculated with both sets of parameters. Indexing the pattern obtained in this study gave $a_o = 6.079$ and $c_o = 8.410$ Å.

Three spinels with 1:3 ordering on the octahedral sites were studied. The details of the preparation of $LiAl_5O_8$, $LiFe_5O_8$, and $LiGa_5O_8$ are given in Table IX. Both ordered and disordered (spinel) polymorphs of $LiAl_5O_8$ and $LiFe_5O_8$ were prepared. The order–disorder transition in $LiAl_5O_8$ occurs at 1295°C (*7*) and in $LiFe_5O_8$ at 735°C (*16*). It was not possible to prepare a disordered form of $LiGa_5O_8$ as Datta and Roy (*8*) have noted, although Joubert (*15*) found the transition at 1140° by DTA. X ray diffraction patterns were in agreement with previous literature. Accurate intensity measurements to determine the degree of disorder in the ordered compounds were not attempted.

Most infrared spectra were obtained by a Beckman IR-11 spectrophotometer. An appropriate amount of finely ground powder in each case was spread uniformly over the surface of a polyethylene plate. The high frequency region of some compounds was measured on a Perkin Elmer 621 Grating Infrared Spectrophotometer using CsI pellets.

The Raman spectra were obtained using both the 488 and 514.5 nm lines of a 200 mW ionized argon laser source and a Spex Ramalog Spectrometer. Powders were pressed into pellets and several spots on each pellet was measured to avoid polarization effects.

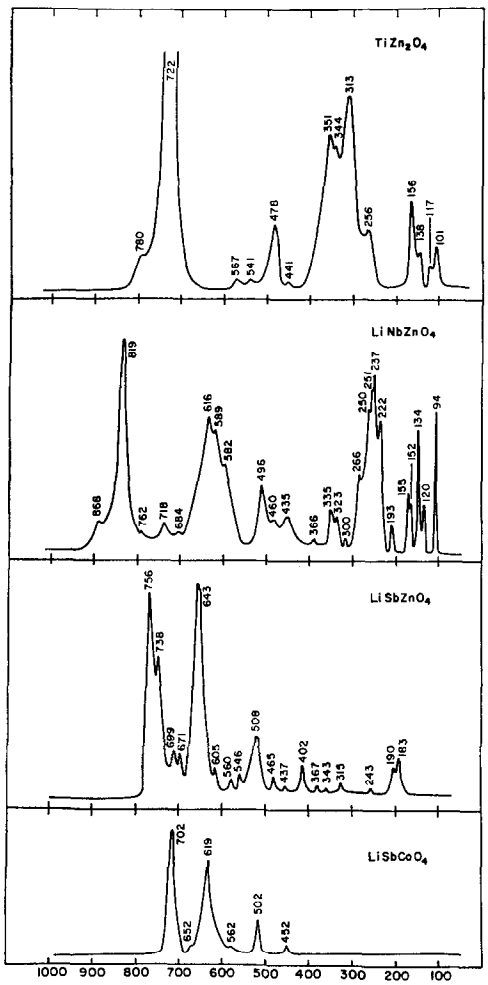

FIG. 3. Raman spectra for spinels with 1:1 order on the octahedral sites.

Results

The infrared spectra of the compounds with 1:1 order are shown in Fig. 2 and the Raman spectra are shown in Fig. 3. The four IR bands observed in the spectra of spinels are replaced by a large number of fairly sharp bands. Perhaps the most striking thing about the IR spectra of Fig. 2 is their dissimilarity. The spectrum of $LiNbZnO_4$ is the most complex with 18 bands, most of similar intensity. The other D_4^3 structure, $TiZn_2O_4$ exhibits much less detail; only six bands are discernible, four of which appear as shoulders on two broad peaks centered at 590 and 396 cm^{-1}. The similarity with $LiNbZnO_4$ is only suggested by the broad minima in the envelope of $LiNbZnO_4$ bands at 590 and 370 cm^{-1} which correspond to similarly placed minima in $TiZn_2O_4$. The Raman spectrum of $LiNbZnO_4$ exhibits some very sharp bands at low frequencies and somewhat broadened ones at high frequencies. Twenty-seven bands are observed and many of these are so closely spaced that resolution of additional features would be difficult. The

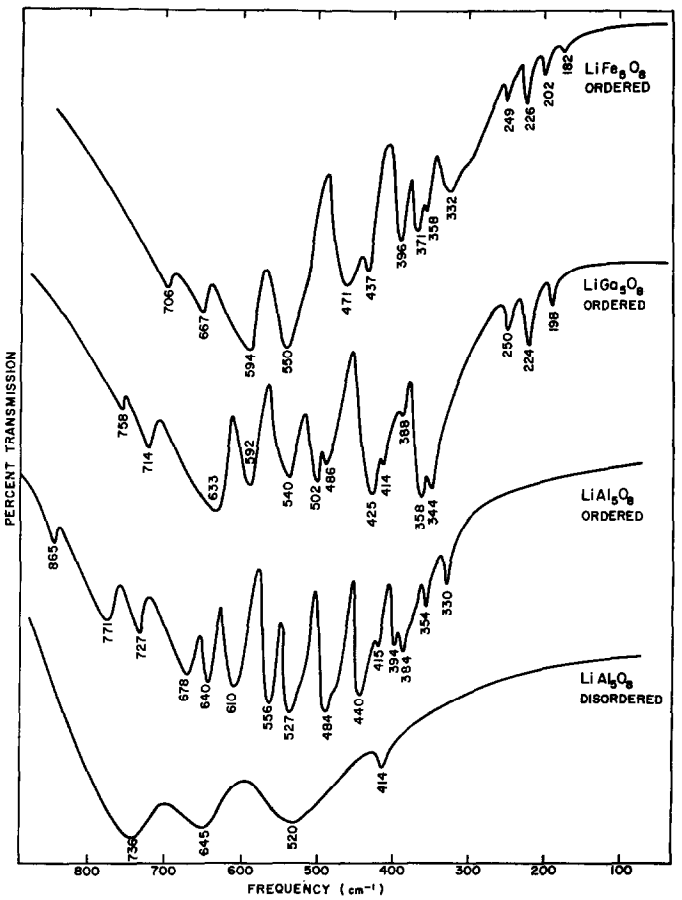

Fig. 4. IR spectra for spinels with 1:3 order on the octahedral sites.

spectrum of $TiZn_2O_4$ is less well defined and only 14 bands are observed.

The IR spectra of $LiSbZnO_4$ and $LiSbCoO_4$ are very similar to each other but distinctly different from the spectra of $LiNbZnO_4$ and $TiZn_2O_4$, as would be expected from the different space group. Nine bands are observed in $LiSbZnO_4$ and 10 bands in $LiSbCoO_4$. The Raman spectrum of $LiSbZnO_4$ is sharp and distinct with 18 bands observed. The Raman spectrum of $LiSbCoO_4$ is similar but with most of the weaker bands absent. The compound is highly colored and selfabsorption of the Raman radiation is a difficult problem.

The results presented above may be compared with the IR spectra of Brabers (*17*) for $TiZn_2O_4$ and $LiNbZnO_4$. Braber's spectra are similar to those shown in Fig. 2 but differ in detail. They extend only to 200 cm^{-1} and so do not include the lowest frequency bands in $LiNbZnO_4$.

Infrared spectra of spinels with 1:3 order on the octahedral sites are shown in Fig. 4 and the Raman spectra in Fig. 5. The IR spectrum of the disordered (spinel-structure) polymorph of $LiAl_5O_8$ exhibits four bands as predicted by factor group analysis. Disordered $LiFe_5O_8$ (not shown) likewise exhibits broad bands centered at 582, 470, and 400 cm^{-1}. The spectra of the ordered structures exhibit closely spaced sharp bands of roughly equal intensity spanning the same frequency range as the spectra of the disordered forms. There are 15, 15, and 14 bands for the aluminate, gallate, and ferrite, respectively, along with several apparent shoulders that could not be resolved.

The details of the spectra, particularly the degree of resolution of the bands, are sensitive to the method of preparation to some extent. The band frequencies change little, but relative intensities vary considerably. This point was not investigated in detail but would be worthy of further experiments, particularly with compounds made with different starting materials and methods of synthesis. The Raman spectra of the ordered compounds consist of fairly sharp lines of varying intensity. There is no obvious pattern or obvious relation to the spectra of the parent spinels. We observe 16, 10, and 14 lines for the aluminate, gallate, and ferrite, respectively. There is no direct correspondence between the Raman and IR frequencies. The Raman spectrum of disordered $LiAl_5O_8$ was measured but is not shown. It was very weak with only two broadened bands at 370 and 740 cm^{-1} superimposed on a background continuum.

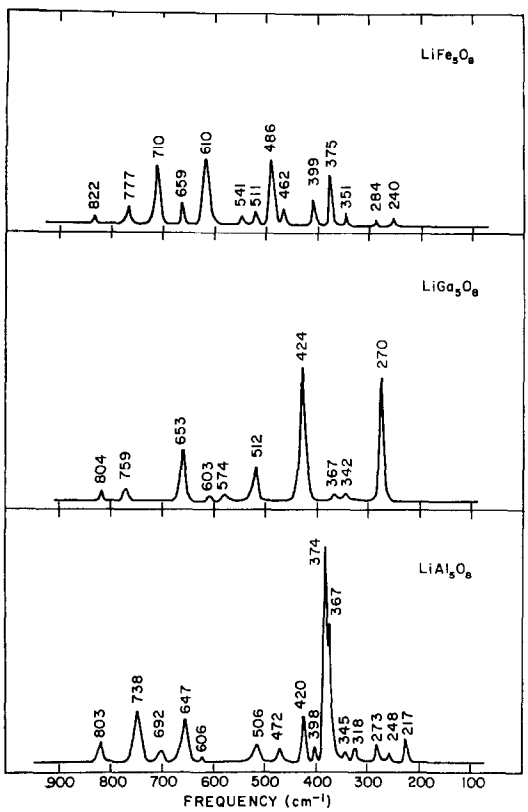

FIG. 5. Raman spectra for spinels with 1:3 order on the octahedral sites.

The impressive fine structure in the IR spectrum of ordered $LiAl_5O_8$ was noted by Hafner and Laves (*18*) and Datta and Roy (*7*). The IR spectra of both $LiAl_5O_8$ and $LiFe_5O_8$ above 300 cm^{-1} were also examined by Tarte and Collongues (*19–23*). The agreement between the earlier measurements and those reported here is quite good except for small changes in relative intensity. It has been argued (*7*) that the order–disorder phase transition is first order and involves an abrupt change from complete disorder to a highly ordered state. Whether the small variations in the infrared spectra imply variations in the state of order according to the method of preparation should be considered as a possibility.

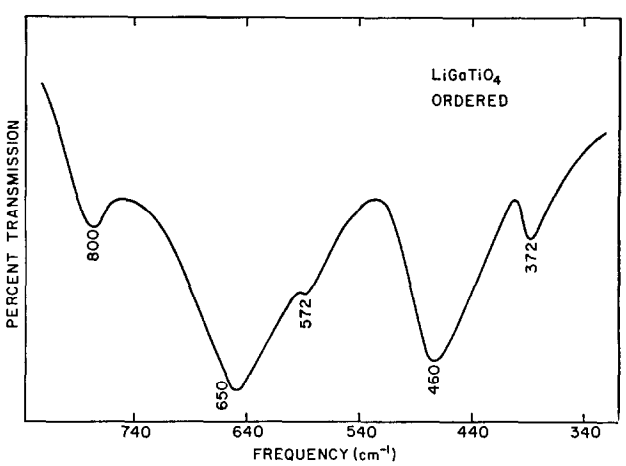

Fig. 6. IR spectrum of ordered $LiGaTiO_4$.

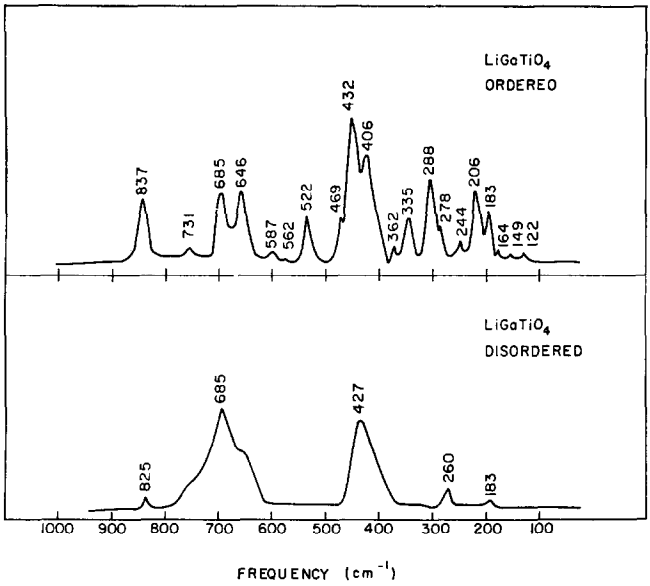

Fig. 7. Raman spectra of ordered and disordered forms of $LiGaTiO_4$

The IR spectrum of $LiGaTiO_4$ in Fig. 6 and Raman spectra of both the ordered and the disordered form are shown in Fig. 7. The IR spectrum is essentially that of a spinel despite the ordering. This behavior is similar to that of $TiZn_2O_4$ where little splitting is observed in the IR, although much detail appears in the Raman. However, the Raman spectrum does show very clearly the effects of ordering. Of the 40 modes predicted to be Raman-active, 20 are observed. The disordered form shows the five peaks expected of a spinel. The disordered compound may actually be partially ordered, because a few extra peaks are beginning to appear as shoulders. The general features of the parent structure are still evident in the spectrum of the ordered form. The two major peaks at 440 and 698 cm^{-1} have now split. Another consequence of the ordering is that some bands exhibit a trend towards higher frequencies.

Discussions and Conclusions

The general characteristics of the vibrational spectra of the ordered spinels may be summarized as follows:

(i) Structural order results in the introduction of many new modes in both IR and Raman spectra. However, the total number predicted by factor group analysis is not usually observed (Table X). A similar result was found in the vibrational spectra of other ordered oxides (*24*).

(ii) The IR bands of the ordered structures are much narrower than the broad bands of the parent spinel. Linewidths of Raman bands are similar in both ordered and disordered structures.

(iii) Intensities of all bands are of comparable magnitude. There is no obvious relationship between strong bands in the ordered structures with those of the parent spinel in those compounds where a comparison can be made.

(iv) Sharp bands appear in both IR and Raman at substantially higher frequencies than any of the bands of the parent spinel.

(v) In two of the compounds, $TiZn_2O_4$ and $LiGaTiO_4$, the infrared spectrum of the ordered structure exhibits little additional detail, whereas the Raman spectrum contains many additional bands.

Examination of the group theoretical calculations and selection rules shows that three crystallographic factors are responsible for

TABLE X

COMPARISON OF OBSERVED MODES FOR THE DIFFERENT ORDERING SCHEMES

Compound	IR		Raman		c/a
	Predicted	Observed	Predicted	Observed	
$LiSbCoO_4$	20	10	15	6	1.001
$LiSbZnO_4$	20	9	15	18	1.001
$LiNbZnO_4$	31	18	50	26	0.98
$TiZn_2O_4$	31	6	50	14	0.99
$LiAl_5O_8$	21	15	40	16	1.00
$LiFe_5O_8$	21	14	40	10	1.00
$LiGa_5O_8$	21	15	40	14	1.00
$LiGaTiO_4$	54	5	40	20	1.00

the large number of predicted IR and Raman modes.

(i) The ordered structures have lower symmetry than the parent structure. The distortion produced by the lower symmetry lifts some of the degeneracy of the cubic structure modes.

(ii) The lower factor group symmetry also relaxes the selection rules, so that inactive modes in the parent structure become allowed in the ordered structures.

(iii) The formation of a superstructure with an enlarged unit cell introduces more degrees-of-freedom and thus more normal modes.

Table X shows that the c/a ratios for both tetragonal and orthorhombic structure are very close to unity if the calculations are made on the pseudocubic spinel cell. The modes separated by distortion will have different selection rules, for they will correspond to motions along the different crystallographic axes of the low symmetry cells. Since all measurements were made on powders, the polarization dependence of the derivative modes was not observed. The frequency difference due to distortion is likely to be very small, and the band splitting may not be observable in the powder spectra. This may account for many of the missing modes.

If the ordering process is assumed to be only a small perturbation on the spinel structure, it can be argued that bands allowed by selection rule relaxation due to ordering will be weak. This was found to be the case with spinels with 1:1 ordering on the tetrahedral sites (*3*) where selection rule relaxation was the only effect of ordering. In this case, the predicted bands were observed but with low intensities compared with those of the parent spinel. However, strong coupling occurred and large frequency shifts were observed. However, weak bands could be lost in the much more complex spectra observed in the present study.

It can be concluded that the discrepancy between the factor group predictions and the number of observed modes can be accounted for if it is assumed that the predicted effects of distortion are not actually observed in the spectra of powders. The main source of the complex set of new bands in the spectra of the ordered compounds arises because of the superstructure.

A structural argument such as was used for the tetrahedral site orderings (*3*) would be to say that the different parts of the superstructure cell are strongly coupled. Since many of the modes have the same symmetry, they would be expected to interact strongly and thus separate in frequency. This argument is more or less an extension of the concept of factor group splitting to superstructures. Some evidence for this explanation is provided by the spectra of $LiNbZnO_4$ and $TiZn_2O_4$. In the first case, the interaction on the octahedral sites is between a monovalent (Li^+) and a pentavalent (Nb^{5+}) ion and the IR spectrum shows many bands well separated in frequency and therefore well resolved. In the second case the interaction is between a divalent (Zn^{2+}) and tetravalent (Ti^{4+}) ion. The interaction energy is smaller and the band separation is

small enough that the individual peaks are not resolved. The long range interaction in the unit cell also appears in the symmetry coordinates (Table VI) which have lost all resemblance to those of the parent spinel structure.

A better way of expressing this long range interaction is provided by the large-zone concept used to analyze the infrared and Raman spectra of the SiC polytypes (*5–7*). Doubling the unit cell in a particular crystallographic direction is equivalent to halving the Brillouin zone. Phonons corresponding to high densities of states at the zone-boundary become zone center phonons in the superstructure and are thus permitted to appear in the IR and Raman spectra. The selection rules for these new modes are given by the factor group analysis of the superstructure. Since the densities of states at the zone boundaries are likely to be comparable to those at the zone center, the intensity of the modes derived from the zone boundary would be of the same magnitude as those from the zone center.

Each zone center phonon of the parent structure will connect to zone boundary phonons in different crystallographic directions. If the dispersion along these related branches is unequal, the set of zone boundary phonons will appear in the superstructure spectrum as well resolved bands. The frequencies depend on the details of the dispersion relations and therefore some may not be resolved if their frequencies are similar and some may be at frequencies considerably removed from the zone-center frequency of the parent structure.

The highest energy zone boundary phonons usually occur at higher frequencies than the corresponding zone-center phonons. The high frequency bands observed in most compounds can thus be accounted for.

There is the problem of the difference in line widths between the IR spectra of the ordered and disordered compounds. The line shapes of infrared bands measured on powders are distorted. The peak does not correspond to the transverse optic mode frequency but instead occurs somewhere between the transverse and longitudinal optic mode frequencies depending on the details of particle size and dielectric constant of the containing medium (*28*). The broad band observed spans most of the interval between ν_t and ν_l. The narrow band widths in the IR spectra of most of the ordered compounds suggest that the longitudinal optic branches have also been folded in the large zone and that the ν_t–ν_l separation has been greatly reduced. It is significant that the two compounds whose IR spectra exhibit little detail are titanates. The long range polarization field in most titanate compounds is exceptionally large.

Acknowledgments

This work was supported by the Air Force Materials Laboratory, Wright Patterson Air Force Base, under Contract No. F33615-69-C-1105 and in part by the Atomic Energy Commission under Contract AT(30-1)-2581.

References

1. C. HAAS, *J. Phys. Chem. Solids* **26**, 1225 (1965).
2. Y. BILLIET, I. MORGENSTERN-BADARAU, AND A. MICHEL, *Bull. Soc. franc. mineral. Crist.* **90**, *8* (1967).
3. B. A. DEANGELIS, V. G. KERAMIDAS, AND W. B. WHITE, *J. Solid State Chem.* **3**, 358 (1971).
4. P. TARTE AND J. PREUDHOMME, *Spectrochim. Acta* **29A**, 1301 (1973).
5. Y. BILLIET AND P. POIX, *Bull. Soc. Chim. France* **1967**, 215 (1967).
6. G. BLASSE, *Philips Res. Rept. Suppl. No. 3* (1964).
7. R. K. DATTA AND R. ROY, *J. Amer. Ceram. Soc.* **36**, 388 (1963).
8. R. K. DATTA AND R. ROY, *J. Amer. Ceram. Soc.* **51**, 297 (1968).
9. E. F. BERTAUT AND G. PATRAT, *Bull. Soc. franc. mineral Crist.* **88**, 586 (1965).
10. W. B. WHITE AND B. A. DEANGELIS, *Spectrochim. Acta* **23A**, 985 (1967).
11. J. PREUDHOMME AND P. TARTE, *Spectrochim. Acta* **27A**, 961, 845, 1817 (1971); **28A**, 69 (1972).
12. V. G. KERAMIDAS, B. A. DEANGELIS, AND W. B. WHITE (to be published).
13. B. A. DEANGELIS, R. E. NEWNHAM, AND W. B. WHITE, *Amer. Mineral.* **57**, 265 (1972).
14. B. A. DEANGELIS, Ph.D. Dissertation, The Pennsylvania State University (1969).
15. J.-C. JOUBERT, Ph.D. Thesis, Faculte des Sciences de l'Universite de Grenoble (1965).
16. P. B. BRAUN, *Nature* **70**, 1123 (1952).
17. V. A. M. BRABERS, *Phys. stat. sol.* (a) **12**, 629 (1972).
19. P. TARTE, *Compt. Rend.* **254**, 2008 (1962).

20. R. COLLONGUES, *Ann. Chim.* **8**, 395 (1963).
21. P. TARTE AND R. COLLONGUES, *Ann. Chim.* **9**, 135 (1964).
22. P. TARTE, *Spectrochim. Acta* **23A**, 2127 (1967).
23. P. TARTE, *Mém. Acad. Roy. Belg.* **35**, 4a, b (1964).
24. W. B. WHITE AND V. G. KERAMIDAS, *Nat. Bur. Standards Spec. Pub.* **364**, 113 (1972).
25. L. PATRICK, *Phys. Rev.* **167**, 809 (1968).
26. D. W. FELDMAN, J. H. PARKER, JR., W. J. CHOYKE, AND L. PATRICK, *Phys. Rev.* **170**, 698 (1968).
27. D. W. FELDMAN, J. H. PARKER, JR., W. J. CHOYKE, AND L. PATRICK, *Phys. Rev.* **173**, 787 (1968).
28. J. D. AXE AND G. D. PETTIT, *Phys. Rev.* **151**, 676 (1966).